Time-step constraints in transient coupled finite element analysis

*W. Cui *, K.A. Gawecka, D.M.G. Taborda, D.M. Potts and L. Zdravković*

Civil and Environmental Engineering, Imperial College London

** w.cui11@imperial.ac.uk (corresponding author)*

Abstract

In transient finite element (FE) analysis, reducing the time-step size improves the accuracy of the solution. However, a lower bound to the time-step size exists, below which the solution may exhibit spatial oscillations at the initial stages of the analysis. This numerical 'shock' problem may lead to accumulated errors in coupled analyses. To satisfy the non-oscillatory criterion, a novel analytical approach is presented in this paper to obtain the time-step constraints using the θ-method for the transient coupled analysis, including both heat conduction-convection and coupled consolidation analyses. The expressions of the minimum time-step size for heat conduction-convection problems with both linear and quadratic elements reduce to those applicable to heat conduction problems if the effect of heat convection is not taken into account. For coupled consolidation analysis, time-step constraints are obtained for three different types of elements and the one for composite elements matches that in the literature. Finally, recommendations on how to handle the numerical 'shock' issues are suggested.

1 Introduction

When the finite element method (FEM) is adopted to obtain approximate solutions in transient analysis (e.g. heat transfer, consolidation, etc.), the differential equation describing the transient problem is first integrated using a finite element discretisation to approximate the numerical solutions in space. Subsequently, a time marching scheme (e.g. the θ-method) is required to approximate the numerical solution over a time interval Δt.

It is generally believed that decreasing the size of the time-step improves the accuracy of the FE solutions to transient problems. However, numerical analyses of consolidation (e.g. [1-6]) as well as heat conduction problems (e.g. [6-10]) have shown that a lower limit for the size of the time-step exists, below which the solution may exhibit spatial oscillations at the initial stages of the analysis in the regions where the gradient of the solution is steep. These oscillations decay and finally disappear as the gradient of the solution reduces. This type of problem is known as a numerical 'shock' problem and is generally induced by a sudden change between the initial and the boundary conditions [11]. For a purely thermal or hydraulic analysis, the issue of oscillations may not be of extreme significance, as the effects are relatively short term and the numerical solution finally becomes accurate (i.e. equal to the analytical solution for simple problmes). However, in an analysis where the hydraulic or thermal behaviour can affect the mechanical response, the final solution may be invalidated, as the errors in the prediction of the mechanical behaviour induced by the oscillations may

accumulate. Therefore, it is necessary to investigate the lower limit of the time-step size in a transient analysis.

The 'hydraulic shock' problem, i.e. the spatial oscillations of pore water pressure in consolidation analysis, has been observed by [1] and [2], and was later studied by [3], who proposed a minimum time-step size for one-dimensional (1D) consolidation of a saturated porous material with an incompressible fluid. The authors derived an expression in terms of material properties and element size for the lower bound of the time-step size, using elements with linear shape functions of pore pressures, and suggested using the same expression with a different multiplier for elements where pore pressures vary quadratically. However, the time-step constraints required for coupled consolidation analysis need further research in order to establish expressions for situations where different combinations of displacement shape functions and pore pressure shape functions are adopted.

The 'thermal shock' problem for heat conduction analysis has also been investigated. [7] used the Discrete Maximum Principle (DMP) to formulate an expression, which is similar to that of [3], for the minimum time-step size for a 1D linear element. [10] and [12] derived the same expression for linear elements adopting a different analytical approach. Although the time-step constraints for the FE analysis of heat conduction problems have been well established in the literature, most of the work has been restricted to analyses using linear elements. Quadratic elements, which are often preferred in geotechnical engineering, have not been extensively investigated. [9] and [13] noted that the DMP may not be sufficient to ensure the non-oscillatory criterion for higher-order finite elements, such as quadratic elements. [10] suggested a more restrictive condition for the minimum time-step size for quadratic elements based on the analytical study for linear elements. However, the process of deriving the equation for quadratic elements was not explained in detail. Therefore, analytical investigation on the time-step constraints for heat conduction analysis with quadratic elements is still required.

In many geotechnical problems, such as open-loop ground source energy systems, a coupled thermo-hydraulic (TH) analysis, including both heat conduction-convection analysis and coupled consolidation analysis, is necessary, meaning that both 'hydraulic shock' and 'thermal shock' may occur. Compared with the heat conduction analysis, an additional convective term, which represents the coupled effect of water flow on total heat transfer, is introduced into the governing equation for heat convection-conduction analysis, and the DMP, as well as other analytical methods in the literature, is not valid even when linear elements are used. Therefore, a new analytical approach is required to obtain the time-step constraints for heat conduction-convection analysis with both linear and quadratic elements.

This paper first presents the non-oscillatory criteria for establishing the time-step constraints for 1D problems. A novel analytical approach is proposed based on the non-oscillatory criteria considering both linear and quadratic elements, and is then applied to both heat conduction-convection and coupled consolidation analyses. Although 1D solutions are less applicable to practical scenarios, further research of 1D problems is still required, especially for higher-order elements and coupled analyses. Also, thorough understanding of the analytical approach for 1D problems is necessary for the investigation of 2D problems, which was found to be more complex in preliminary studies carried out by the authors. The expressions derived analytically in this paper are validated against analyses performed using

the Imperial College Finite Element Program – ICFEP [14], which is capable of simulating the fully coupled thermo-hydro-mechanical (THM) behaviour of porous materials. The integration scheme used in all numerical analysis presented in this paper is the θ-method, which is unconditionally stable when values of θ are greater or equal to 0.5 [15].

2 Time-step constraints for FE analysis of heat conduction-convection

2.1 Mathematical description of a 1D heat conduction-convection analysis

The basic function governing total heat transfer in soils can be written as:

$$\frac{\partial(\Phi dV)}{\partial t} + \nabla \cdot Q dV = 0 \qquad (1)$$

where Φ is the heat content of the soil per unit volume, Q is the heat flux per unit volume, including heat conduction and heat convection, t is the time, and dV is the volume of the material. Considering 1D heat conduction-convection, Equation (1) can be rewritten as:

$$\rho C_p \frac{\partial T}{\partial t} - k_\theta \frac{\partial^2 T}{\partial x^2} + \rho_w C_{pw} v_w \frac{\partial T}{\partial x} = 0 \qquad (2)$$

where the first term on the left-hand side represents the heat content of the soil, with ρ and C_p being the density and the specific heat capacity of the soil, respectively, and the second and the last terms represent heat conduction and heat convection, respectively, with v_w being the velocity of the pore fluid. For a saturated soil, ρC_p can be expressed in terms of its components as:

$$\rho C_p = n\rho_w C_{pw} + (1-n)\rho_s C_{ps} \qquad (3)$$

where n is the porosity, and the subscripts w and s denote pore water and soil particles respectively.

To investigate the 'thermal shock' problem in an analysis of heat conduction-convection, a generalised one-dimensional mesh, with a total length of L and composed of n elements with a length of h, is considered (as shown in Figure 1).The following boundary conditions are applied at the ends of the mesh

$$T(0,t) = T_b\,,\ \frac{\partial T}{\partial x}(L,t) = 0 \qquad (4)$$

which represent a constant temperature, T_b, specified at the left-hand end and no heat flux at the right-hand end of the mesh. The initial condition is $T(x,0) = T_0$, where T_0 is assumed to be lower than T_b. To include convective heat transfer, a water flow from left to right along the bar is applied with a velocity of v_w.

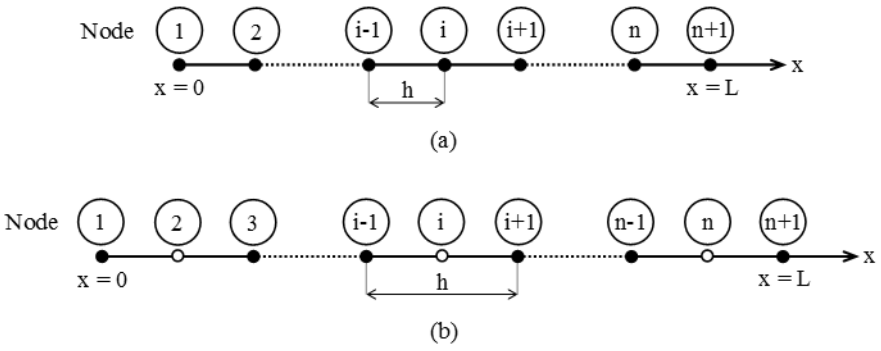

Figure 1 One-dimensional representation of the mesh with (a) linear elements and (b) quadratic elements

For the analysis of 1D heat conduction-convection shown above, spatial oscillations in nodal temperature can be observed at the initial stage if the time-step size is not sufficiently large. To avoid oscillations, the following two non-oscillatory criteria on the temperature at node *i* at time *t*, $T_i = T(x_i, t)$ should be satisfied when heating:

1) $T_i \geq T_0$ for any $t \geq 0$ (i.e. the temperature change at any node should not be negative);
2) $T_i \leq T_{i-1}$ (i.e. that the temperature variation should decrease monotonically along the bar).

2.2 Minimum time-step size for linear elements

When linear elements are adopted in a FE analysis of the above heat conduction-convection problem, Equation (2) can be discretized using the Galerkin method, resulting in:

$$\begin{cases} \int_{x_i}^{x_{i+1}} \left[k_\theta \frac{dN_i}{dx}\left(\frac{dN_i}{dx}T_i + \frac{dN_{i+1}}{dx}T_{i+1}\right) + \rho C_p N_i\left(N_i\frac{\partial T_i}{\partial t} + N_{i+1}\frac{\partial T_{i+1}}{\partial t}\right) + \rho_w C_{pw} v_w N_i\left(\frac{dN_i}{dx}T_i + \frac{dN_{i+1}}{dx}T_{i+1}\right)\right] dx = 0 \\ \int_{x_i}^{x_{i+1}} \left[k_\theta \frac{dN_{i+1}}{dx}\left(\frac{dN_i}{dx}T_i + \frac{dN_{i+1}}{dx}T_{i+1}\right) + \rho C_p N_{i+1}\left(N_i\frac{\partial T_i}{\partial t} + N_{i+1}\frac{\partial T_{i+1}}{\partial t}\right) + \rho_w C_{pw} v_w N_{i+1}\left(\frac{dN_i}{dx}T_i + \frac{dN_{i+1}}{dx}T_{i+1}\right)\right] dx = 0 \end{cases} \quad (5)$$

Substituting the shape functions of linear elements into Equation (5) and then evaluating the integrals, yields:

$$[C_l]\cdot\left\{\frac{\partial T}{\partial t}\right\} + ([K_l] + [D_l])\cdot\{T\} = \{0\} \quad (6)$$

with the boundary conditions as $T_1 = T_b$ and $\partial T_{n+1}/\partial x = 0$ for any $t > 0$, and the initial conditions as $T_i = T_0$ at $t = 0$ for any $1 \leq i \leq n+1$. For linear elements, the matrix $[C_l]$, which represents the heat content of the material, and the matrices $[K_l]$ and $[D_l]$, which represent the heat transfer due to conduction and convection respectively, can be assembled from the elemental matrices resulting in:

$$[C_l]=\frac{h}{6}\begin{bmatrix}2&1&0&...&...&...\\1&4&1&0&...&...\\0&1&4&1&0&...\\...&...&...&...&...&...\\...&...&0&1&4&1\\...&...&...&0&1&2\end{bmatrix},[K_l]=\frac{\alpha}{h}\begin{bmatrix}1&-1&0&...&...&...\\-1&2&-1&0&...&...\\0&-1&2&-1&0&...\\...&...&...&...&...&...\\...&...&0&-1&2&-1\\...&...&...&0&-1&1\end{bmatrix}, \text{ and}$$

$$[D_l]=\frac{\rho_w C_{pw} v_w}{2\rho C_p}\begin{bmatrix}-1&1&0&...&...&...\\-1&0&1&0&...&...\\0&-1&0&1&0&...\\...&...&...&...&...&...\\...&...&0&-1&0&1\\...&...&...&0&-1&1\end{bmatrix}$$

As spatial oscillations are of higher importance at the beginning of the analysis, the nodal temperatures T_i after the first time-step, Δt, will be investigated here. According to the finite difference discretisation, the following relationship can be established:

$$\frac{\partial T}{\partial t}=\frac{\Delta T}{\Delta t}=\frac{T_i-T_0}{\Delta t} \qquad (7)$$

Moreover, given that the θ-method is adopted, Equation (6) must be observed for $t = \theta\Delta t$, for which the corresponding temperature can be calculated using:

$$T=\theta T_i+(1-\theta)T_0 \qquad (8)$$

Substituting equations (7) and (8) into Equation (6) results in:

$$\left[\frac{1}{\theta\Delta t}[C_l]+([K_l]+[D_l])\right](\{T_i\}-\{T_0\})=-\frac{1}{\theta}([K_l]+[D_l])\{T_0\} \qquad (9)$$

If the same initial temperature is applied to all nodes, as in the analysed case, substituting the matrices $[K_l]$ and $[D_l]$ results in the right-hand side in Equation (9) reducing to zero. Therefore, Equation (9) can be written as a linear system of the form:

$$[A_l]\cdot\{\Delta T\}=\{0\} \qquad (10)$$

where

$$[A_l]=\frac{1}{\theta\Delta t}[C_l]+([K_l]+[D_l]) \qquad (11)$$

Substituting the matrices $[C_l]$, $[K_l]$ and $[D_l]$ into Equation (11) yields:

$$[A_l]=\frac{\alpha}{6h}\begin{bmatrix} 6+\frac{2}{\theta F_0}-3Pe & -6+\frac{1}{\theta F_0}+3Pe & 0 & 0 & ... \\ -6+\frac{1}{\theta F_0}-3Pe & 12+\frac{4}{\theta F_0} & -6+\frac{1}{\theta F_0}+3Pe & 0 & ... \\ ... & ... & ... & ... & ... \\ ... & 0 & -6+\frac{1}{\theta F_0}-3Pe & 12+\frac{4}{\theta F_0} & -6+\frac{1}{\theta F_0}+3Pe \\ ... & 0 & 0 & -6+\frac{1}{\theta F_0}-3Pe & 6+\frac{2}{\theta F_0}+3Pe \end{bmatrix}$$

where $F_0 = k_\theta \Delta t/(\rho C_p h^2)$ is the Fourier number, which can be considered to represent the maximum temperature gradient in the domain for transient heat transfer problems [9], and $Pe = \rho_w C_{pw} v_w h/k_\theta$ is defined as the Péclet number which represents the ratio between the convective and the conductive transport rates.

For the analysis of 1D heat conduction (without convection) using linear elements, [7] and [8, 9] applied the Discrete Maximum Principle (DMP) to establish the time-step constraint that satisfies the non-oscillatory criterion. The DMP requires that for a linear system given by Equation (10) [16]:

1) the matrix $[A_l]$ is invertible and has a dominant diagonal;
2) all the diagonal terms of $[A_l]$ are positive and the non-diagonal terms are non-positive.

However, applying the Discrete Maximum Principle to the heat conduction-convection problem, a strict condition of $Pe < 2$ is obtained in order to ensure that the non-diagonal term $-6+1/(\theta F_0)+3Pe$ is non-positive, which means that the DMP is violated for any analysis with $Pe \geq 2$. Therefore, to obtain a general time-step constraint for the heat conduction-convection analysis with any value of Pe, an alternative novel analytical approach is introduced here.

For the analysis of heat conduction-convection with linear elements, expanding the linear system given by Equation (10) leads to:

$$\frac{\alpha}{6h}\begin{bmatrix} 6+\frac{2}{\theta F_0}-3Pe & X+3Pe & ... & ... & ... & ... \\ X-3Pe & 12+\frac{4}{\theta F_0} & X+3Pe & ... & ... & ... \\ ... & X-3Pe & 12+\frac{4}{\theta F_0} & X+3Pe & ... & ... \\ ... & ... & ... & ... & ... & ... \\ ... & ... & ... & X-3Pe & 12+\frac{4}{\theta F_0} & X+3Pe \\ ... & ... & ... & ... & X-3Pe & 6+\frac{2}{\theta F_0}+3Pe \end{bmatrix}\begin{Bmatrix} \Delta T_1 \\ \Delta T_2 \\ \Delta T_3 \\ ... \\ \Delta T_n \\ \Delta T_{n+1} \end{Bmatrix}=\begin{Bmatrix} 0 \\ 0 \\ 0 \\ 0 \\ 0 \\ 0 \end{Bmatrix}$$

(12)

where $X = -6+1/(\theta F_0)$. Investigations on the above linear system with the prescribed boundary conditions have shown that the non-oscillatory condition is governed by the last two nodes along the bar. To ensure that the non-oscillatory conditions are satisfied at every node along the bar, it should be observed that the incremental temperature change, at the

node furthest away from the node where a higher temperature has been prescribed, must be non-negative (i.e. $\Delta T_{n+1} \geq 0$). Moreover, a monotonic reduction in temperature must take place, meaning that the temperature at the final node must be less or equal to the temperature at the previous node (i.e. $T_{n+1} \leq T_n$). Analysing the last row from Equation (12) gives:

$$(6+\frac{2}{\theta F_0}+3Pe)\Delta T_{n+1} = (6-\frac{1}{\theta F_0}+3Pe)\Delta T_n \qquad (13)$$

Applying the restriction $\Delta T_{n+1} \geq 0$ leads to:

$$6-\frac{1}{\theta F_0}+3Pe \geq 0 \qquad (14)$$

Applying the second restriction $T_n/T_{n+1} \geq 1$, or equally $\Delta T_n/\Delta T_{n+1} \geq 1$, since all nodes have the same initial temperature which ensures a monotonically decreasing temperature distribution along the bar, to Equation (13) also yields the same condition as that shown by Equation (14). Therefore, it can be concluded that for the 1D analysis of heat conduction-convection with linear elements, both of the non-oscillatory criteria can be satisfied simultaneously when the condition given by Equation (14) is satisfied.

Solving the inequality given by Equation (14), a minimum size of time-step is obtained for heat conduction-convection analysis with linear elements, and it can be written as:

$$\Delta t \geq \frac{\rho C_p h^2}{3\theta k_\theta (2+Pe)} \qquad (15)$$

To verify the above time-step constraints, an analysis of the 1 m long bar with element lengths of 0.1 m shown in Figure 2 was carried out in ICFEP using the material properties of a typical sandstone (listed in Table 1). The initial temperature was 0 °C and a fixed temperature boundary condition (T = 10 °C) was prescribed on the left-hand end of the mesh. To include the convective heat transfer, a constant pore water pressure gradient was applied over the mesh to induce a constant water flow from left to right with a velocity of 5.9×10^{-6} m/s. Additionally, a coupled thermo-hydraulic boundary condition was prescribed on both ends of the mesh to account for the heat transfer induced by the water entering and leaving the mesh. The θ-method was applied with the backward difference scheme (θ = 1.0), and linear elements were employed in the analysis. It should be noted that, although the problem is discretised in 2D (i.e. the elements used in the finite element analysis are quadrilateral), a 1D heat and pore water flow is ensured by specifying suitable boundary condition, hence verification of the analytical expressions is possible.

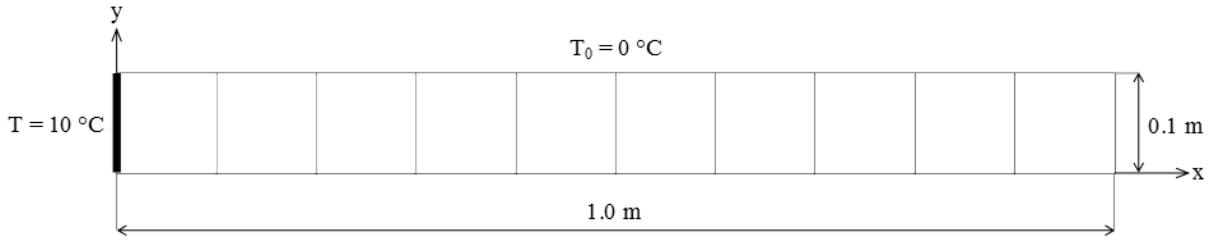

Figure 2 Finite element mesh and thermal boundary conditions

Table 1 Material properties for heat transfer analysis

Density of solids, ρ_s (t/m^3)	2.5
Density of water, ρ_w (t/m^3)	1.0
Specific heat capacity of solids, C_{ps} (kJ/t.K)	880
Specific heat capacity of water, C_{pw} (kJ/t.K)	4190
Thermal conductivity, k_θ (kJ/s.m.K)	0.001
Void ratio, e	0.3

For this exercise, the critical time-step required for the non-oscillatory condition can be calculated from Equation (15) as: Δt_{cr} = 1980 s. Figure 3 shows a close-up of the temperature distribution along the first elements of the mesh after one increment, with time-steps of 1960 s ($\Delta t < \Delta t_{cr}$) and 2000 s ($\Delta t > \Delta t_{cr}$). The analysis with the time-step of 1960 s, which is only slightly below the critical time-step, exhibits spatial oscillations of temperature as the temperature at the second node (x = 0.1 m) is negative, which is also less than the temperature at the third node (x = 0.2 m). However, when the time-step of 2000 s was used, both of the non-oscillatory criteria were satisfied simultaneously.

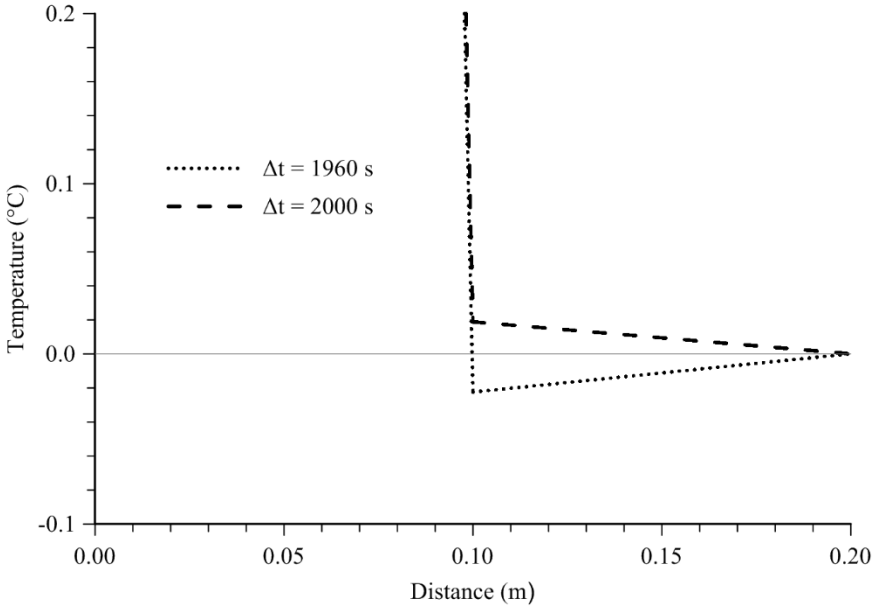

Figure 3 Nodal temperatures up to 0.2 m along the bar at increment 1 in the simulation of heat conduction-convection using linear elements

2.3 Minimum time-step size for quadratic elements

A similar procedure has been applied to investigate the time-step constraints which should be satisfied in order to avoid spatial oscillations using quadratic elements. Discretising Equation (2), using the Galerkin method and carrying out the integration, results in a similar expression to Equation (6), where the matrices $[C_q]$, $[K_q]$ and $[D_q]$ for quadratic elements can be written, respectively, as:

$$\left[K_q\right]=\frac{\alpha}{3h}\begin{bmatrix} 7 & -8 & 1 & ... & ... & ... \\ -8 & 16 & -8 & 0 & ... & ... \\ 1 & -8 & 7 & -8 & 1 & ... \\ ... & ... & ... & ... & ... & ... \\ ... & ... & 0 & -8 & 16 & -8 \\ ... & ... & ... & 1 & -8 & 7 \end{bmatrix}, \left[C_q\right]=\frac{h}{15}\begin{bmatrix} 2 & 1 & -1/2 & ... & ... & ... \\ 1 & 8 & 1 & 0 & ... & ... \\ -1/2 & 1 & 4 & 1 & -1/2 & ... \\ ... & ... & ... & ... & ... & ... \\ ... & ... & 0 & 1 & 8 & 1 \\ ... & ... & ... & -1/2 & 1 & 2 \end{bmatrix}$$

$$\text{and } \left[D_q\right]=\frac{\rho_w C_{pw} v_w}{6\rho C_p}\begin{bmatrix} -3 & 4 & -1 & ... & ... & ... \\ -4 & 0 & 4 & 0 & ... & ... \\ 1 & -4 & 0 & 4 & -1 & ... \\ ... & ... & ... & ... & ... & ... \\ ... & ... & 0 & -4 & 0 & 4 \\ ... & ... & ... & 1 & -4 & 3 \end{bmatrix}$$

Applying the θ-method and noting that the for a constant initial temperature distribution the term $([K_q]+[D_q])\{T_0\}$ is zero, a linear system similar to Equation (10) is obtained, where the matrix $[A_q]$ for quadratic elements can be expressed as:

$$\left[A_q\right]=\frac{\alpha}{h}\begin{bmatrix} a-\frac{Pe}{2} & b+\frac{2Pe}{3} & c-\frac{Pe}{6} & 0 & ... & ... \\ b-\frac{2Pe}{3} & d & b+\frac{2Pe}{3} & 0 & ... & ... \\ c+\frac{Pe}{6} & b-\frac{2Pe}{3} & e & b+\frac{2Pe}{3} & c-\frac{Pe}{6} & ... \\ ... & ... & ... & ... & ... & ... \\ & & & b-\frac{2Pe}{3} & d & b+\frac{2Pe}{3} \\ & & & c+\frac{Pe}{6} & b-\frac{2Pe}{3} & a+\frac{Pe}{2} \end{bmatrix}$$

where

$$a=\frac{7}{3}+\frac{2}{15\theta F_0}, \qquad b=-\frac{8}{3}+\frac{1}{15\theta F_0}, \qquad c=\frac{1}{3}-\frac{1}{30\theta F_0},$$

$$d=\frac{16}{3}+\frac{8}{15\theta F_0}, \qquad e=\frac{14}{3}+\frac{4}{15\theta F_0}$$

For the analysis of 1D heat conduction (without convection), [9] and [13] noted that the criterion derived from the Discrete Maximum Principle may not be sufficient to ensure adequate results for high-order finite elements. Applying the DMP to the above linear system for quadratic elements, the condition of $Pe < 2$ is also required to ensure that the non-diagonal terms in $[A_q]$ are non-positive. Alternatively, the proposed approach for linear elements is adopted here to investigate the minimum time-step size for quadratic elements.

Expanding the linear system for quadratic elements gives:

$$\frac{\alpha}{h}\begin{bmatrix} a-\frac{Pe}{2} & b+\frac{2Pe}{3} & c-\frac{Pe}{6} & \dots & \dots & \dots \\ b-\frac{2Pe}{3} & d & b+\frac{2Pe}{3} & 0 & \dots & \dots \\ c+\frac{Pe}{6} & b-\frac{2Pe}{3} & e & b+\frac{2Pe}{3} & c-\frac{Pe}{6} & \dots \\ \dots & \dots & \dots & \dots & \dots & \dots \\ \dots & \dots & 0 & b-\frac{2Pe}{3} & d & b+\frac{2Pe}{3} \\ 0 & \dots & \dots & c+\frac{Pe}{6} & b-\frac{2Pe}{3} & a+\frac{Pe}{2} \end{bmatrix}\begin{Bmatrix} \Delta T_1 \\ \Delta T_2 \\ \Delta T_3 \\ \dots \\ \Delta T_n \\ \Delta T_{n+1} \end{Bmatrix}=\begin{Bmatrix} 0 \\ 0 \\ 0 \\ 0 \\ 0 \\ 0 \end{Bmatrix} \qquad (16)$$

Following a similar process to the one presented for linear elements and analysing the last two rows from Equation (16) and eliminating ΔT_{n-1} leads to:

$$\frac{\Delta T_n}{\Delta T_{n+1}}=\frac{\left(b-\frac{2Pe}{3}\right)\left(a+\frac{Pe}{2}\right)-\left(b+\frac{2Pe}{3}\right)\left(c+\frac{Pe}{6}\right)}{d\left(c+\frac{Pe}{6}\right)-\left(b-\frac{2Pe}{3}\right)^2} \qquad (17)$$

Applying to Equation (17) the restriction $\Delta T_n/\Delta T_{n+1} \geq 0$, which ensures the temperature change at any node is non-negative, yields:

$$\Delta t \geq \frac{\rho C_p h^2}{2\theta k_\theta\left(7+Pe+\sqrt{169+74Pe+11Pe^2}\right)} \qquad (18)$$

Conversely, applying to Equation (17) the restriction $\Delta T_n/\Delta T_{n+1} \geq 1$, which ensures monotonically decreasing temperature along the bar, yields:

$$\Delta t \geq \frac{3\rho C_p h^2}{20\theta k_\theta\left(3+Pe\right)} \qquad (19)$$

Comparing the two expressions above, it can be shown that the value returned by Equation (19) is always greater than that given by Equation (18). Therefore, the time-step constraint which satisfies both of the non-oscillatory criteria is defined by Equation (19).

For the previously presented example of conduction-convection analysis using quadratic elements, the critical time-step required for the criterion of non-negative incremental change can be calculated from Equation (18) as: Δt_{cr1} = 444 s. Figure 4 shows a close-up of the temperature distribution along the bar after one increment, with time-steps of 420 s ($\Delta t < \Delta t_{cr1}$) and 460 s ($\Delta t > \Delta t_{cr1}$). It can be seen that using a time-step size slightly above that critical value can avoid the negative incremental temperature change. However, spatial oscillations still exist as the temperature at the second node (x = 0.05 m) is lower than that at the third node (x = 0.10 m).

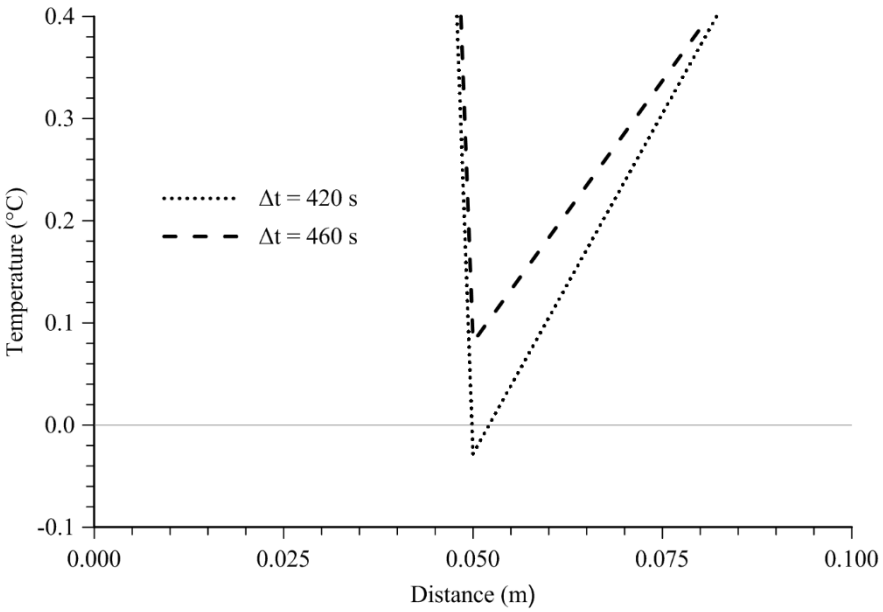

Figure 4 Nodal temperatures up to 0.1 m along the bar at increment 1 in the simulation of heat conduction-convection using quadratic elements

The critical time-step required to satisfy both of the non-oscillatory criteria can be calculated from Equation (19) as: Δt_{cr} = 729 s. To validate it, exercises of solving the linear system given by Equation (13), with the prescribed boundary conditions and the material properties listed in Table 1, were first carried out. Two time-step sizes of 700 s and 740 s were adopted and the temperatures at the nodes next to the right-hand end of the bar (0.75 m $\leq$ x $\leq$ 1.00 m) are listed in Table 2. It can be seen that with a time-step slightly larger than that critical value, a monotonically decreasing temperature distribution can be observed as the nodal temperature at the last node (x = 1.00 m) is lower than that at the preceding node (x = 0.95 m). However, in the case with Δt = 700 s (i.e. less than Δt_{cr}) oscillations at the last two nodes exist. Figure 5 shows the monotonically decreasing temperature distribution along the bar with a time-step size of 740 s.

Table 2 Nodal temperatures at increment 1 in the solution of the heat conduction-convection problem using quadratic elements

x (m)	T (°C)	
	Δt = 700 s	Δt = 740 s
0.75	1.870E-10	1.704E-10
0.80	1.203E-10	9.380E-11
0.85	8.068E-12	7.128E-12
0.90	5.205E-12	3.935E-12
0.95	**3.398E-13**	**2.926E-13**
1.00	**3.841E-13**	**2.800E-13**

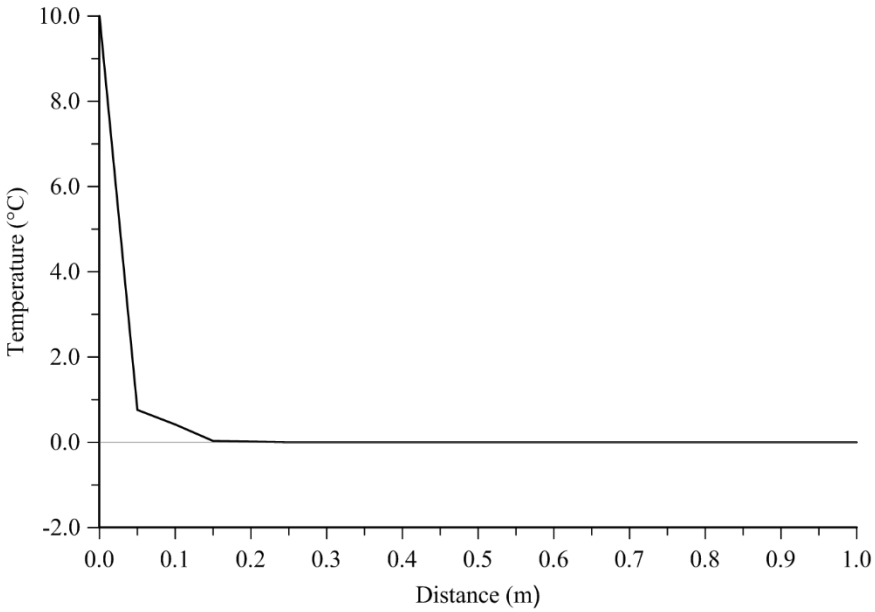

Figure 5 Nodal temperatures at increment 1 with Δt = 740s in the simulation of heat conduction-convection using quadratic elements

2.4 A special case of heat conduction

For an analysis of 1D heat conduction (*Pe* = 0) with linear elements, Equation (15) reduces to:

$$\Delta t \geq \frac{\rho C_p h^2}{6\theta k_\theta} \qquad (20)$$

The same time-step constraint has also been shown by [10] and [12]. It should be noted that applying the DMP also leads to the same time constraint as that given by Equation (20) for heat conduction analysis with linear elements [7, 8].

When quadratic elements are used in the analysis of heat conduction, the time-step constraint given by Equation (18), which ensures that the incremental temperature change at any node is non-negative, reduces to:

$$\Delta t \geq \frac{\rho C_p h^2}{40\theta k_\theta} \qquad (21)$$

while the time-step constraint given by Equation (19), which satisfies both of the non-oscillatory criteria and leads to a monotonic temperature distribution along the bar, can be reduced to:

$$\Delta t \geq \frac{\rho C_p h^2}{20\theta k_\theta} \qquad (22)$$

It should be noted that applying the DMP can only lead to the condition given by Equation (21), which demonstrates that the DMP is insufficient to ensure the non-oscillatory conditions for the analysis of heat conduction with quadratic elements, in agreement with the conclusions drawn by [9]. For the heat conduction analysis using quadratic elements with the mesh shown in Figure 2 and the material properties listed in Table 1, the minimum time-step

size which only satisfies the criterion of non-negative incremental temperature change can be calculated from Equation (21) as: $\Delta t_{cr1} = 665$ s. The validity of this critical time-step can be verified by comparing FE results with two time-step sizes of 650 s and 680 s as shown in Figure 6.

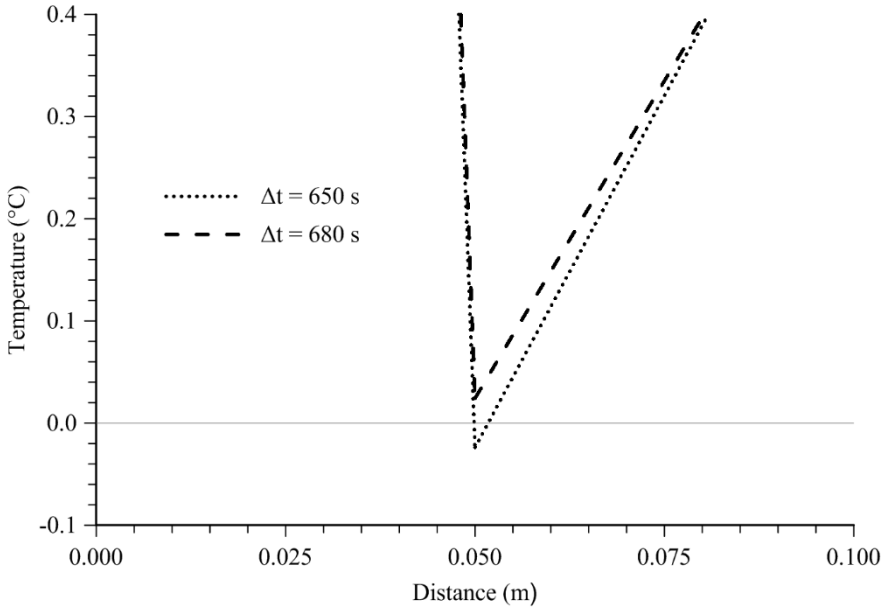

Figure 6 Nodal temperatures up to 0.1 m along the bar at increment 1 in the simulation of heat conduction using quadratic elements

The minimum time-step size which satisfies both of the non-oscillatory criteria can be calculated from Equation (22) as: $\Delta t_{cr} = 1330$ s. Validation exercises similar to that for heat conduction-convection problems were performed. The nodal results listed in Table 3 show that when the time-step size is less than the critical one, oscillations at the last two nodes are present, however, in the case with $\Delta t_{cr} = 1350$ s, monotonically decreasing temperature along the bar can be observed (Figure 7).

Table 3 Nodal temperatures at increment 1 in the solution of the heat conduction problem using quadratic elements

x (m)	T (°C)	
	Δt = 1300 s	Δt = 1350 s
0.75	3.546E-10	3.551E-10
0.80	1.936E-10	1.804E-10
0.85	1.624E-11	1.612E-11
0.90	8.886E-12	8.209E-12
0.95	**7.779E-13**	**7.650E-13**
1.00	**8.122E-13**	**7.438E-13**

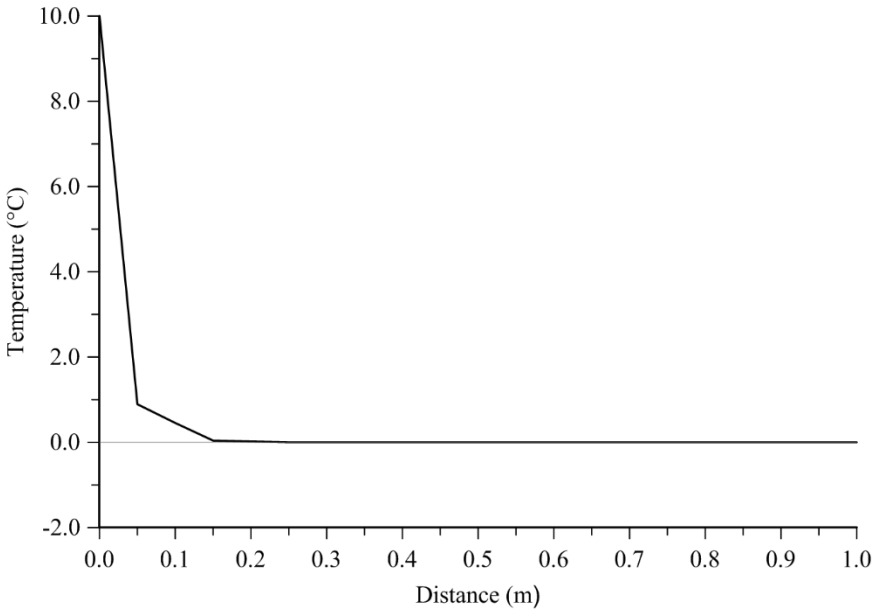

Figure 7 Nodal temperatures at increment 1 with Δt = 1350s in the simulation of heat conduction using quadratic elements

3 Time-step constraints for FE analysis of coupled consolidation

3.1 Mathematical description of the 'hydraulic shock' problem

For an incompressible fluid, the pore water flow in soils is governed by the continuity equation, which can be written as [14]:

$$\frac{\partial v_x}{\partial x} + \frac{\partial v_y}{\partial y} + \frac{\partial v_z}{\partial z} - Q^w = \frac{\partial \varepsilon_v}{\partial t} \qquad (23)$$

where v_x, v_y, v_z are the components of the velocity of the pore water in the coordinate directions, ε_v is the volumetric strain of the soil skeleton, and Q^w represents any pore water sources and/or sinks. The seepage velocity $\{v_w\}^T = \{v_x, v_y, v_z\}$ is considered to be governed by the Darcy's law given by:

$$\{v_w\} = -[k_w]\nabla h_w \qquad (24)$$

where h_w is the hydraulic head defined as:

$$\{h_w\} = -\frac{\nabla p_f}{\gamma_f} - [k_w]\{i_G\} \qquad (25)$$

where p_f is the pore water pressure, $[k_w]$ is the permeability matrix, γ_f is the specific weight of the pore water, and the vector $\{i_G\}^T = \{i_{Gx}, i_{Gy}, i_{Gz}\}^T$ is the unit vector parallel, but in the opposite direction, to gravity. If neither the effect of gravity nor the fluid source/sink term is taken into account, Equation (23) can be rewritten as:

$$\frac{\partial \varepsilon_v}{\partial t} - \frac{k_w}{\gamma_f}\frac{\partial^2 p_f}{\partial x^2} = 0 \qquad (26)$$

It is noted that the term containing volumetric strain in Equation (26) represents the coupled effect of the mechanical behaviour on the pore water flow.

To represent the 'hydraulic shock' problem in coupled consolidation analysis, a generalised 1D mesh, with the total length of L and composed of n elements of a length of h, is considered (shown in Figure 1). A higher pore water pressure is prescribed at the left-hand end and no change in pore water pressure was prescribed at the right-hand end of the bar. A 1D deformation of the bar is enforced by specifying suitable mechanical boundary conditions. In order to obtain the time-step constraints for coupled consolidation analysis following a similar procedure to that outlined for heat conduction-convection analysis, it is necessary to replace the volumetric strain in Equation (26) by a term which includes pore water pressures. Alternative scenarios using finite elements with three different combinations of displacement shape function and pore water pressure shape function are considered in the following sections.

3.2 Minimum time-step size

3.2.1 Composite elements

In consolidation analyses, it is common to use composite elements where pore water pressure varies linearly across the element, whereas displacement varies quadratically [17]. In this case, quadratic shape functions are used to interpolate displacements and linear shape functions are used to interpolate pore water pressures. In a finite element analysis of the 1D consolidation problem described above, the volumetric strain is given for this type of element by:

$$\{\Delta\varepsilon_v\} = \{\Delta\varepsilon\} = [B]\{\Delta d\}_n \qquad (27)$$

where $[B]$ is the matrix which contains only derivatives of the shape functions and $\{\Delta d\}_n$ is the vector of nodal displacement. Therefore, the volumetric strain varies with the same order as the pore water pressure across the element and can be calculated as:

$$\varepsilon_v = \frac{p_f}{M_c} \qquad (28)$$

where M_c is the constrained modulus, which can be written as:

$$M_c = \frac{1-v}{(1+v)(1-2v)}E \qquad (29)$$

with E being Young's modulus and v the Poisson's ratio.

Substituting Equation (28) into Equation (26) yields:

$$\frac{\partial p_f}{\partial t} - \frac{k_w M_c}{\gamma_f}\frac{\partial^2 p_f}{\partial x^2} = 0 \qquad (30)$$

Clearly, Equation (30) has the same form as the partial differential equation for heat conduction, and therefore the same procedure for derivation of the minimum time-step size for linear elements can be followed, leading to:

$$\Delta t \geq \frac{\gamma_f h^2}{6\theta M_c k_w} \qquad (31)$$

It should be noted that the same minimum time-step size was given by [3], who started the process directly from Equation (30) without describing which type of shape function was used for displacements. The effect of loading can be taken into account by following a similar process as shown by [3].

3.2.2 Other types of elements

In geotechnical engineering, it is also possible to simulate coupled consolidation problems with two other types of elements: standard linear elements and standard quadratic elements. As using both of these elements leads to an equation which is different from Equations (28), time-step constraints, which are different from that obtained by [3], can be obtained following an approach similar to that proposed in this paper for heat conduction-convection problems.

In standard linear elements, both the displacement and the pore water pressure vary linearly across an element. For such an element, the volumetric strain is constant over the element due to the linear relations adopted in the shape functions for the displacements. Therefore, in the one-dimensional exercise of a coupled consolidation analysis with linear elements, the elemental volumetric strain $\varepsilon_{v,n}$ can be given as:

$$\varepsilon_{v,n} = \frac{p^*_{f,n}}{M_c} \qquad (32)$$

where $p^*_{f,n}$ is the average pore water pressure of the element.

Substituting Equation (32) into Equation (26) yields:

$$\frac{\partial p^*_{f,n}}{\partial t} - \frac{k_w M_c}{\gamma_f}\frac{\partial^2 p_f}{\partial x^2} = 0 \qquad (33)$$

Discretizing Equation (33) using the Galerkin method and carrying out the integration yields an equation similar to Equation (6), where the matrices $[C_{l,c}]$ and $[K_{l,c}]$, which represent the fluid flow due to the volumetric change of the soil skeleton and the fluid flow due to the gradient of hydraulic head, respectively, can be assembled from the elemental matrices:

$$\left[C_{l,c}\right] = \frac{h}{4}\begin{bmatrix} 1 & 1 & 0 & \dots & \dots & \dots \\ 1 & 2 & 1 & 0 & \dots & \dots \\ 0 & 1 & 2 & 1 & 0 & \dots \\ \dots & \dots & \dots & \dots & \dots & \dots \\ \dots & \dots & 0 & 1 & 2 & 1 \\ \dots & \dots & \dots & 0 & 1 & 1 \end{bmatrix} \text{ and } \left[K_{l,c}\right] = \frac{k_w M_c}{h\gamma_f}\begin{bmatrix} 1 & -1 & 0 & \dots & \dots & \dots \\ -1 & 2 & -1 & 0 & \dots & \dots \\ 0 & -1 & 2 & -1 & 0 & \dots \\ \dots & \dots & \dots & \dots & \dots & \dots \\ \dots & \dots & 0 & -1 & 2 & -1 \\ \dots & \dots & \dots & 0 & -1 & 1 \end{bmatrix}$$

Following a procedure similar to that outlined for heat conduction-convection problems, the lower limit of the time-step size for the 1D coupled consolidation analysis with standard linear elements can be obtained as:

$$\Delta t \geq \frac{\gamma_f h^2}{4\theta M_c k_w} \qquad (34)$$

Table 4 Material properties in consolidation analysis

Young's modulus, E (MPa)	10
Poisson ratio, v (-)	0.3
Permeability, k_w (m/s)	1.0×10^{-8}
Void ratio, e (-)	0.6

To verify the above time-step constraint, a coupled consolidation analysis was conducted with ICFEP. The same mesh as the one shown in Figure 2, with material properties listed in Table 4, was used. However, the prescribed temperature boundary condition was replaced by a prescribed constant pore water pressure of 10 kPa. Additionally, a boundary condition imposing no changes in pore water pressure was prescribed at the right-hand end of the mesh. Displacement boundary conditions were prescribed so that only 1D deformation of the bar was allowed. A zero pore water pressure was applied as the initial condition and the θ-method was employed with the backward difference scheme (θ = 1.0). For this example, the critical time-step for standard linear elements can be calculated from Equation (34) as Δt_{cr} = 182 s. Figure 8 compares the FE results of pore water pressures for $\Delta t < \Delta t_{cr}$ (Δt = 170 s) and $\Delta t > \Delta t_{cr}$ (Δt = 190 s). It can be seen that the spatial oscillations disappear for the second case.

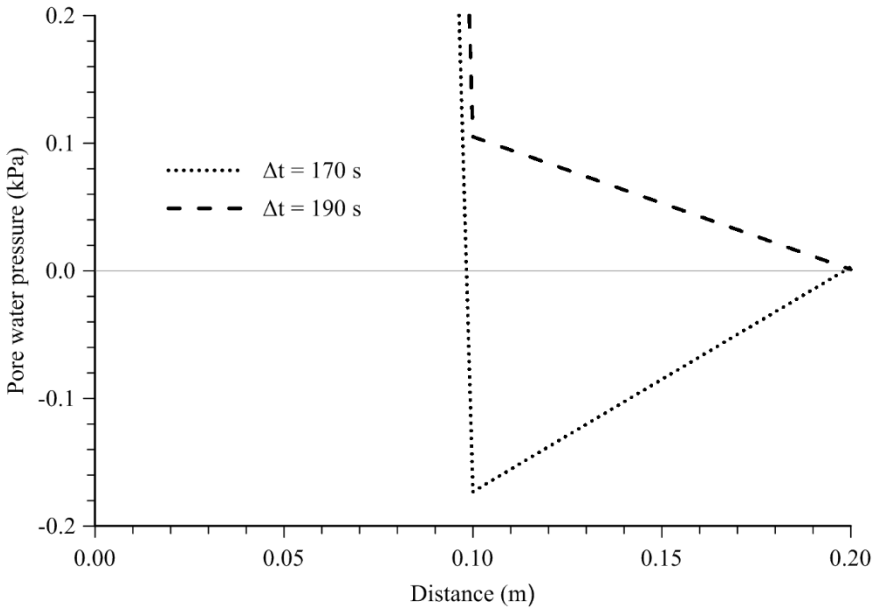

Figure 8 Nodal pore water pressures up to 0.2 m along the bar at increment 1 in a coupled consolidation analysis using standard linear elements

In standard quadratic elements, both the displacements and the pore water pressures vary quadratically, while the volumetric strains vary linearly. For such elements, the behaviour of the quadratic element between two adjacent nodes when simulating the consolidation phenomenon is the same as that of the standard linear element. Therefore, the minimum time-step which satisfies the non-oscillatory conditions for quadratic elements can be obtained from Equation (34) as:

$$\Delta t \geq \frac{\gamma_f (h/2)^2}{4\theta M_c k_w} \qquad (35)$$

or

$$\Delta t \geq \frac{\gamma_f h^2}{16\theta M_c k_w} \qquad (36)$$

Therefore, the critical time-step for the coupled consolidation example above is Δt_{cr} = 45 s. The results of FE analyses with $\Delta t < \Delta t_{cr}$ (Δt = 40 s) and $\Delta t > \Delta t_{cr}$ (Δt = 50 s) are depicted in Figure 9, and show that spatial oscillations disappear for the latter case.

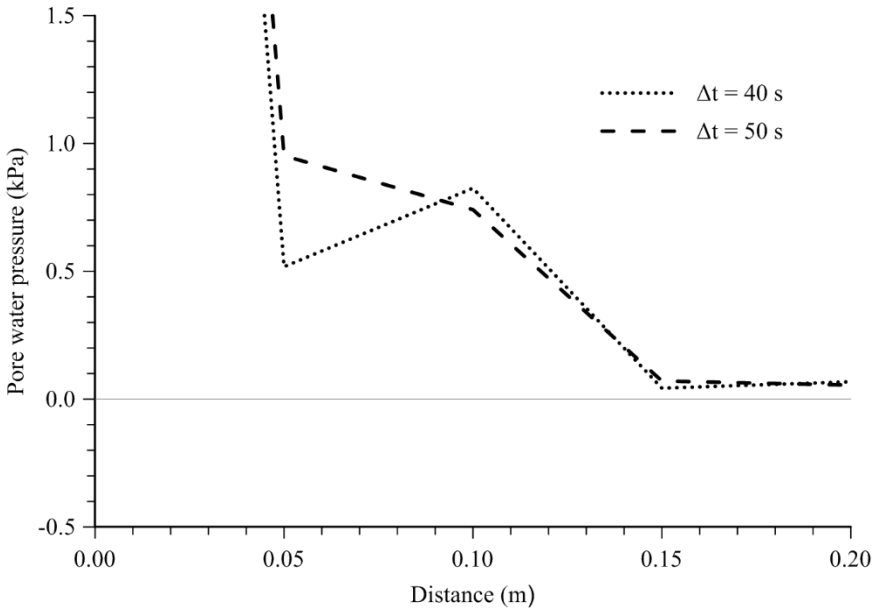

Figure 9 Nodal pore water pressures up to 0.2 m along the bar at increment 1 in a coupled consolidation analysis using standard quadratic elements

4 Recommendations for establishing the critical time-step

To avoid spatial oscillations in the FE analysis of transient problems, a minimum size of the time-step is required, which depends on the material properties and element size. For soils, a large initial time-step is generally necessary in the analysis of thermal shock problems, as porous materials have a lower thermal diffusivity compared to other solids, such as metals. In consolidation analysis, porous materials with lower permeability, e.g. clays, could also require a large initial time-step to satisfy the non-oscillatory conditions. It should be noted that, in some extreme cases, the minimum time-step size calculated using the equations presented in this paper may be too large for accurate solutions to be obtained, and may also affect the accuracy of the solutions to other coupled equations.

To avoid spatial oscillations without adopting an extremely large time-step size, various numerical approaches have been suggested in the literature, such as the mass matrix lumping (e.g. [12]) for heat transfer problems, and a smoothing technique (e.g. [4]) as well as a least-square method (e.g. [18]) for consolidation problems. However, using these methods may change the physical characteristics of the problem and result in a reduction in accuracy [19]. Here, assuming that the governing equations and the matrices obtained using the Galerkin finite element method remain unchanged, two approaches are possible. One is to reduce the time-step constraint by refining the mesh near the boundary where the boundary conditions change. Alternatively, as suggested by [20], the boundary conditions can be applied gradually with respect to the initial conditions. To investigate this latter method, a series of exercises has been performed to illustrate some important aspects of the behaviour of spatial

oscillations caused by numerical shock. Although conduction of heat is considered here, it should be noted that similar results apply to consolidation and heat conduction-convection problems. All of the following analyses are based on the example described for heat conduction analysis, with the mesh shown in Figure 2 and the material properties listed in Table 1. For brevity, only quadratic elements are considered here.

Firstly, the oscillations occur independently of the magnitude of the applied boundary temperature. This can be illustrated by prescribing different temperature change on the left-hand end of the mesh (ΔT_1 = 1, 10 or 100 °C), while the initial temperature, T_0, remains at 0 °C. It can be seen in Figure 10 that the spatial variation after the first time-step of the nodal temperature normalised by the prescribed boundary temperature change is the same for all of the analysed cases.

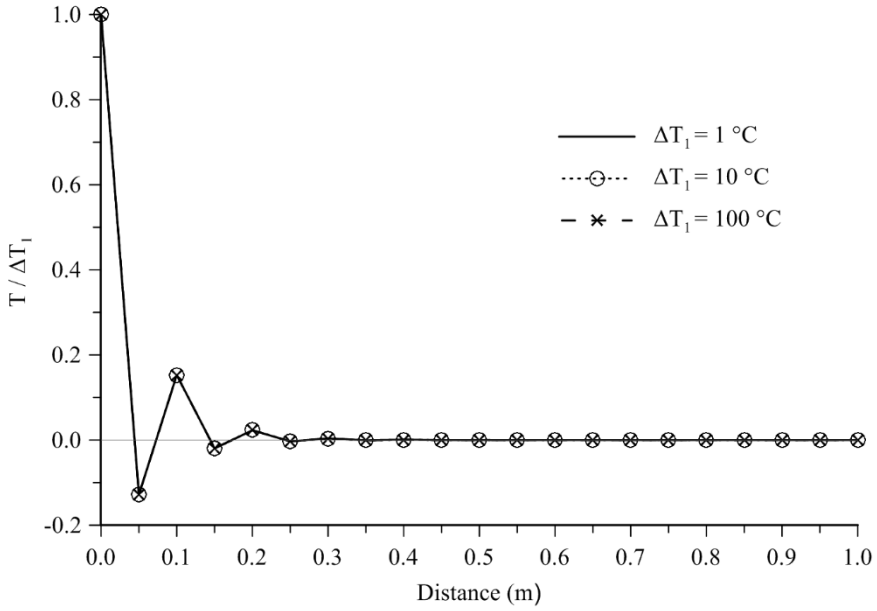

Figure 10 Spatial variation of the normalised nodal temperature at increment 1 using quadratic elements with Δt = 60 s

Secondly, as expected, the magnitude of oscillations after the first increment reduces as the size of the time-step approaches the critical value. This can be seen in Figure 11, where the time-step size was varied between $0.1\Delta t_{cr}$ and Δt_{cr}.

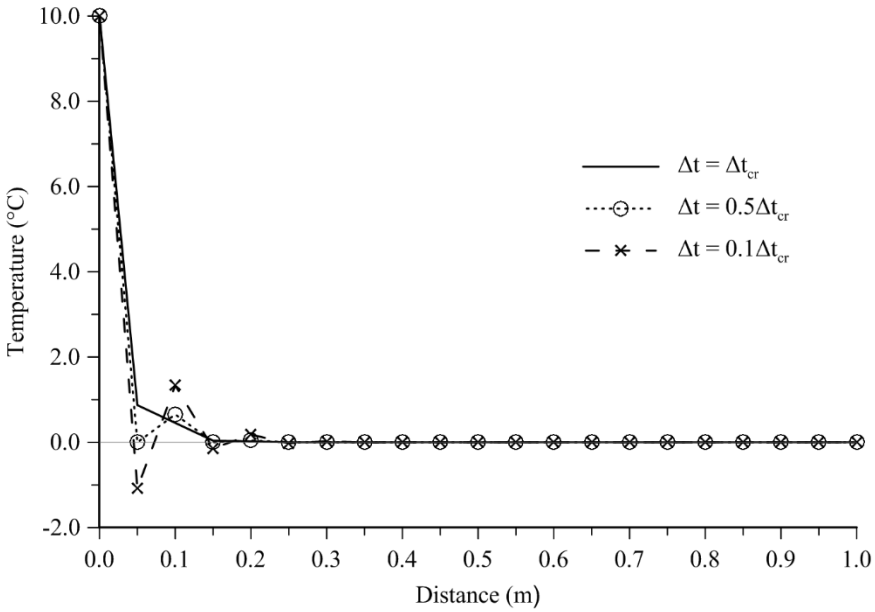

Figure 11 Effect of time-step size on spatial oscillations (increment 1)

Thirdly, the magnitude of the oscillations does not change significantly when the total boundary temperature change is applied gradually over the same total time. This is illustrated by the comparison of numerical results from two exercises presented in Figure 12. In the first exercise, an increase of 10°C is prescribed on the left-hand end of the mesh in the first increment with a time-step of 60 s. Conversely, in the second exercise, a total boundary temperature increase of 10°C is applied in equal steps over the first ten increments (i.e. ΔT_1 =1 °C/INC) with a time-step of 6 s. It should be noted from Figure 12 that although the oscillation in the second exercise is small after the first increment, it accumulates with the incremental change of boundary temperature resulting in larger amplitudes at increment 10.

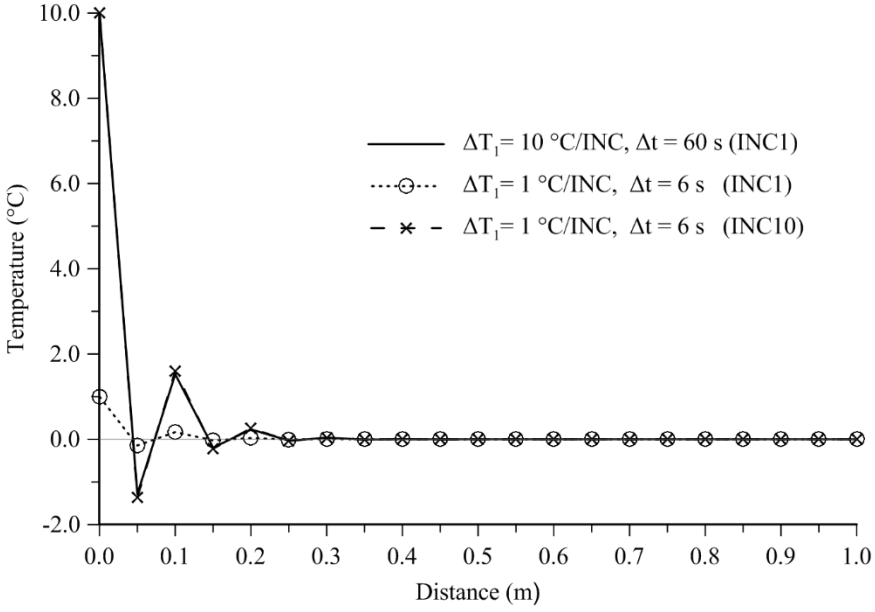

Figure 12 Effect of rate of application of boundary temperature over the same total time

Lastly, the magnitude of oscillations reduces when the total boundary temperature change is applied gradually over a larger total time. This can be illustrated by the comparison of

numerical results from two exercises shown in Figure 13. In the first exercise, an increase of 10°C is prescribed on the left-hand end of the mesh in the first increment (i.e. ΔT_1 =10 °C/INC) with a time-step of 60 s, while in the second exercise a total boundary temperature increase of 10°C is applied in equal steps over the first ten increments (i.e. ΔT_1 =1 °C/INC) with the same time-step of 60 s (600 s in total). It should be noted that in the second exercise the total time, over which the total boundary temperature change is applied, is still smaller than the critical time-step of 1330 s.

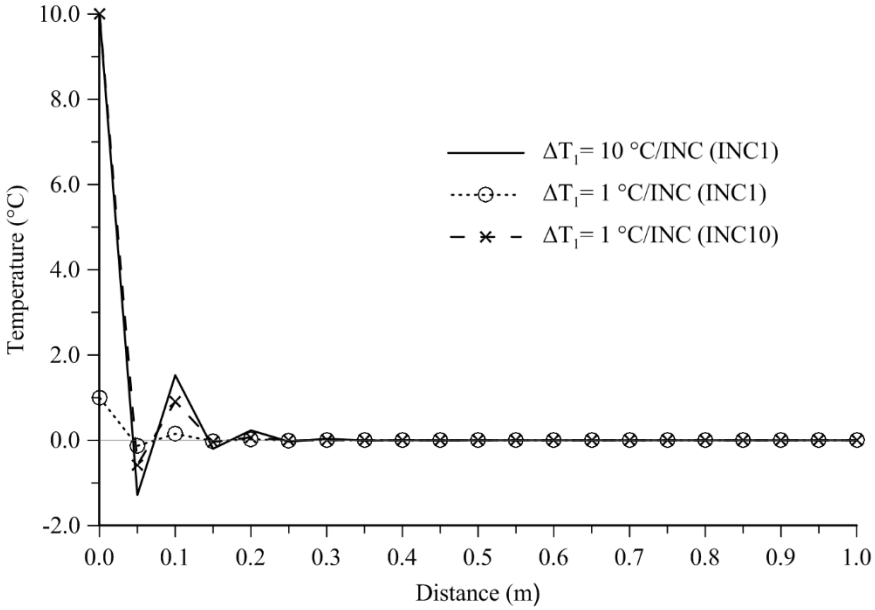

Figure 13 Effect of rate of application of boundary temperature over different total time (Δt = 60 s)

Based on the results obtained from the above exercises, it can be concluded that only increasing the total time-step, over which the boundary conditions are gradually applied, can reduce the spatial oscillations. Therefore, an effective method of reducing the oscillations, as well as avoiding a large time-step size, is to apply the boundary conditions gradually over a total time-step which is equal to the critical value obtained from the expression for the minimum time-step size. To validate this, an additional exercise has been performed where a total boundary temperature increase of 10°C is applied equally over the first ten increments with the incremental time-step of $0.1\Delta t_{cr}$. It can be observed from Figure 14 that, although the oscillations still exist after increment 10, their amplitude has reduced considerably.

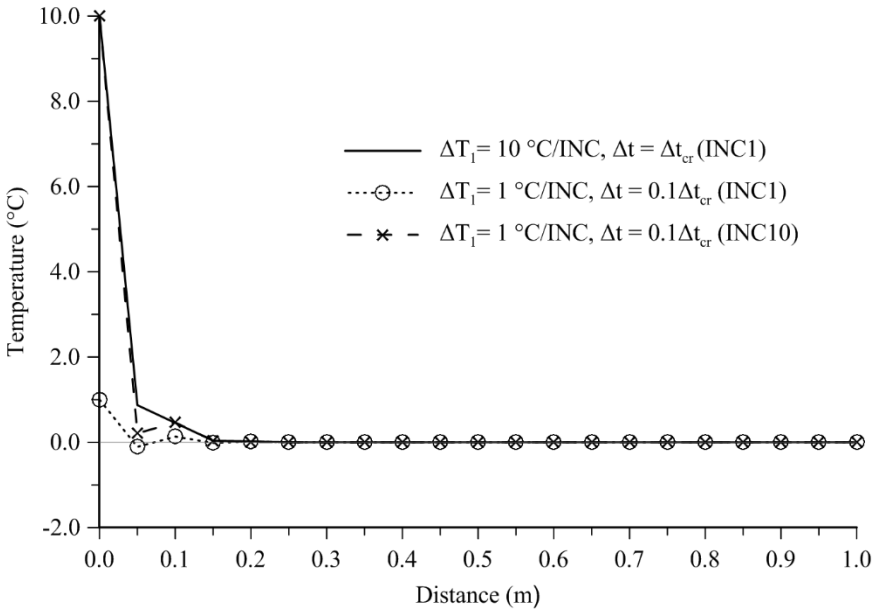

Figure 14 Effect of rate of application of boundary temperature over the total time equal to the critical time-step (Δt_{cr} = 1330 s)

5 Conclusions

This paper investigates the time-step constraints of the θ-method in the FE analysis of transient coupled problems. A novel process for obtaining the minimum size of the time-step required for the FE analysis of 1D heat conduction-convection and coupled consolidation problems with both linear and quadratic elements has been presented respectively. The key conclusions can be summarised as follows:

(1) Adopting the proposed analytical approach, the time-step constraints for the FE analysis of 1D heat conduction-convection problems are established and validated for both linear and quadratic elements. When linear elements are used, both of the non-oscillatory criteria presented in the paper can be satisfied simultaneously once a time-step size larger than the critical one is adopted. When quadratic elements are used, however, the non-oscillatory criterion which ensures the non-negative incremental temperature change is satisfied before the one which ensures monotonic temperature distribution is satisfied. Therefore, an additional lower bound of time-step size corresponding to first non-oscillatory criterion is also analytically derived for quadratic elements.

(2) When there is no water flow, the obtained time-step constraints for heat conduction-convection problems reduce to those for heat conduction. For linear elements, the resulting expression matches the one in the literature which is obtained using the Discrete Maximum Principle. For quadratic elements, it is shown that applying the DMP can only lead to the time-step constraints ensuring a non-negative incremental temperature change at any node along the bar. To avoid spatial oscillations, the proposed analytical process should be applied which results in a more restrictive time-step constraint for quadratic elements.

(3) The same theory is applied to establish the time-step constraints in coupled consolidation analysis using elements with combinations of different types of pore water pressure shape function and displacement shape function. It is shown that the same time-step constraint as

that presented in the literature is derived if the composite elements are adopted. However, using standard linear elements and standard quadratic element will result in a new criterion.

(4) Studies on the behaviour of the spatial oscillations in 1D heat conduction problems have shown that they are independent of the value of the boundary condition applied. In order to reduce the magnitude of the oscillations without refining the mesh or using an extremely large time-step, which could increase the computational effort or reduce the accuracy of the solution, respectively, the total boundary value change should be applied gradually over a total time-step which is equal to the critical time-step.

In the numerical examples presented in this paper, the backward difference scheme ($\theta = 1$) was chosen, however, it should be noted that using different values of θ leads to the same conclusions as the ones reported.

It should also be stressed that, although the numerical analyses were performed using 2D quadrilateral elements, suitable boundary conditions were imposed such that the pore water and/or heat flow were 1D. Hence, verification of the analytical expressions against numerical simulations is possible. Problems, where the pore water and/or heat flow are multidirectional (i.e. 2D or 3D), were found, by the authors, to be more complex and the critical time-step could not be obtained analytically but had to be determined by trial and error (as also noted by [6]), and therefore are not included in this paper. Even though 1D solutions are less applicable to practical scenarios, the authors found that a thorough understanding of the 1D problems is necessary for extending the theory to more dimensions.

Acknowledgements

This research is funded by China Scholarship Council (CSC) and Engineering and Physical Sciences Research Council (EPSRC).

References

1. Yokoo Y, Yamagata K, Nagaoka H. Finite element analysis of consolidation following undrained deformation. *Soils and Foundations* 1971; **11**: 37-58.
2. Sandhu RS, Liu H, Singh KJ. Numerical performance of some finite element schemes for analysis of seepage in porous elastic media. *International Journal for Numerical and Analytical Methods in Geomechanics* 1977; **1**: 177-194.
3. Vermeer PA, Verruijt A. An accuracy condition for consolidation by finite elements. *International Journal for Numerical and Analytical Methods in Geomechanics* 1981; **5**: 1-14.
4. Reed MB. An investigation of numerical errors in the analysis of consolidation by finite elements. *International Journal for Numerical and Analytical Methods in Geomechanics* 1984; **8**: 243-257.
5. Thomas HR, Harb HM. On the use of a standard quadratic element in the analysis of consolidation following external loading. *Communications in Applied Numerical Methods* 1986; **2**: 531-539.
6. Murti V, Valliappan S, Khalili-Naghadeh N. Time step constraints in finite element analysis of the Poisson type equation. *Computers & Structures* 1989; **31**: 269-273.
7. Rank E, Katz C, Werner H. On the importance of the discrete maximum principle in transient analysis using finite element methods. *International Journal for Numerical Methods in Engineering* 1983; **19**: 1771-1782.

8. Lobo M, Emery AF. The discrete maximum principle in finite-element thermal radiation analysis. *Numerical Heat Transfer, Part B: Fundamentals: An International Journal of Computation and Methodology* 1993; **24**: 209-227.
9. Lobo M, Emery AF. Use of the discrete maximum principle in finite-element analysis of combined conduction and radiation in nonparticipating media. *Numerical Heat Transfer, Part B: Fundamentals: An International Journal of Computation and Methodology* 1995; **27**: 447-465.
10. Thomas HR, Zhou Z. Minimum time-step size for diffusion problem in FEM analysis. *International Journal for Numerical Methods in Engineering* 1997; **40**: 3865-3880.
11. Fachinotti VD, Bellet M. Linear tetrahedral finite elements for thermal shock problems. *International Journal of Numerical Methods for Heat & Fluid Flow* 2006; **16**: 590-601.
12. Bergheau JM, Fortunier R. *Finite Element Simulation of Heat Transfer*. Wiley: London, 2008.
13. Vejchodsky T, Solin P. Discrete maximum principle for higher-order finite elements in 1D. *Mathematics of Computation* 2007; **76**: 1833-1846.
14. Potts DM, Zdravković L. *Finite Element Analysis in Geotechnical Engineering: Theory*. Thomas Telford: London, 1999.
15. Booker JR, Small JC. An investigation of the stability of numerical solutions of Biot's equations of consolidation. *International Journal of Solids and Structures* 1975; **11**: 907-917.
16. Ciarlet PG. Discrete maximum principle for finite-difference operators. *Aequationes Mathematicae* 1970; **4**: 338-352.
17. Potts DM, Zdravković L. *Finite Element Analysis in Geotechnical Engineering: Application*. Thomas Telford: London, 2001.
18. Truty A. A Galerkin/least-squares finite element formulation for consolidation. *International Journal for Numerical Methods in Engineering* 2001; **52**: 763-786.
19. Diersch HJ. *FEFLOW: Finite Element Modeling of Flow, Mass and Heat Transport in Porous and Fractured Media*. Springer: Berlin, 2014.
20. Zienkiewicz OC, Taylor RL. *The Finite Element Method: The basis*. Butterworth-Heinemann: Oxford, 2000.

Table 5 Material properties for heat transfer analysis

Density of solids, ρ_s (t/m^3)	2.5
Density of water, ρ_w (t/m^3)	1.0
Specific heat capacity of solids, C_{ps} (kJ/t.K)	880
Specific heat capacity of water, C_{pw} (kJ/t.K)	4190
Thermal conductivity, k_θ (kJ/s.m.K)	0.001
Void ratio, e	0.3

Table 6 Nodal temperatures at increment 1 in the solution of the heat conduction-convection problem using quadratic elements

x (m)	T (°C)	
	$\Delta t = 700$ s	$\Delta t = 740$ s
0.75	1.870E-10	1.704E-10
0.80	1.203E-10	9.380E-11
0.85	8.068E-12	7.128E-12
0.90	5.205E-12	3.935E-12
0.95	**3.398E-13**	**2.926E-13**
1.00	**3.841E-13**	**2.800E-13**

Table 7 Nodal temperatures at increment 1 in the solution of the heat conduction problem using quadratic elements

x (m)	T (°C)	
	Δt = 1300 s	Δt = 1350 s
0.75	3.546E-10	3.551E-10
0.80	1.936E-10	1.804E-10
0.85	1.624E-11	1.612E-11
0.90	8.886E-12	8.209E-12
0.95	**7.779E-13**	**7.650E-13**
1.00	**8.122E-13**	**7.438E-13**

Table 8 Material properties in consolidation analysis

Young's modulus, E (MPa)	10
Poisson ratio, v (-)	0.3
Permeability, k_w (m/s)	1.0×10^{-8}
Void ratio, e (-)	0.6